



Preparation of covalently cross-linked sulfonated polybenzimidazole membranes for vanadium redox flow battery applications



Zijun Xia^{a,b}, Libin Ying^a, Jianhua Fang^{a,*}, Yu-Yu Du^c, Wei-Ming Zhang^{c,*}, Xiaoxia Guo^a, Jie Yin^a

^a Shanghai Electrochemical Energy Devices Research Center, School of Chemistry and Chemical Engineering, Shanghai Jiao Tong University, 800 Dongchuan Road, Shanghai 200240, China

^b GE (China) Research and Development Center Co., Ltd., 1800 Cailun Road, Zhangjiang High-tech Park, Pudong, Shanghai 201203, China

^c College of Chemistry & Materials Engineering, Wenzhou University, Wenzhou 325000, China

ARTICLE INFO

Keywords:

Sulfonated polybenzimidazole
Membrane
Cross-linking
Vanadium permeability
Redox flow battery performance

ABSTRACT

A series of polybenzimidazole copolymers with varied content of pendant amino groups have been synthesized by condensation polymerization of 4,4'-dicarboxydiphenyl ether (DCDPE), 5-aminoisophthalic acid (APTA) and 3,3'-diaminobenzidine (DAB) in polyphosphoric acid at 190 °C for 20 h. The resulting copolymers undergo post-sulfonation in fuming sulfuric acid at 100 °C yielded the highly sulfonated polybenzimidazoles (**SOPBI-NH₂(x/y)**, 'x/y' refers to the monomer molar ratio of DCDPE to APTA). A series of covalently cross-linked membranes (**CSOPBI-NH₂(x/y)**) with good mechanical properties are fabricated by solution cast technique using bisphenol A epoxy resin as a cross-linker. The CSOPBI membranes show 3–4 orders of magnitude lower VO²⁺ permeability and 6–30 times higher ion diffusion selectivity (proton vs. VO²⁺) than Nafion117. The charge-discharge behaviors of the vanadium redox flow batteries (VRBs) assembled with the **CSOPBI-NH₂(x/y)** membranes and Nafion 117 are investigated and compared. The VRBs assembled with the CSOPBI membranes exhibit significantly higher columbic efficiency and lower self-discharge rate than that assembled with Nafion 117 owing to the extremely lower vanadium cations crossover of the former. The VRB assembled with the **CSOPBI-NH₂(9/1)** membrane exhibits fairly high energy efficiency (~85% at 60 mA cm⁻²) and little decay in performance is observed after 300 charge-discharge cycles.

1. Introduction

Since the discovery of vanadium redox flow batteries (VRB) by Sklyllas-Kazacos and co-workers [1,2] in 1985, the VRB has attracted increasing attention owing to its promising applications in medium- and large-scale energy storage. In 1997, a 200 kW VRB stack built by Kashima-Kita was successfully interconnected to the company's power plant grid system [3]. A separator is one of the key components of a VRB system. From viewpoint of practical applications, a separator must meet the requirements of high proton conductivity, little vanadium crossover, good mechanical properties and excellent chemical stability. At present, the most widely used separator in the VRB is DuPont's Nafion[®], a sulfonated perfluorinated polymer membrane which has been widely used in chlor-alkali industry in the past decades. It has the merits of high proton conductivity and excellent chemical stability. However, the high cost and high vanadium permeability which causes serious self-discharge problem restrict their further applications in VRB. It is generally recognized that Nafion[®] possesses perfect nanophase-separated morphology consisting of ionic channels

(1 nm in diameter) interconnecting ionic clusters (4 nm in diameter) which facilitate ionic (protons, vanadium cations, etc.) transport, while the highly hydrophobic Teflon backbone provides Nafion[®] with excellent chemical stability and good mechanical properties [4–6]. To reduce vanadium crossover of Nafion[®], many modification approaches have been developed such as incorporation of amino-silica [6] or layered silicate [7] into Nafion[®] matrix, preparation of composite membrane using porous poly(tetrafluoroethylene) substrate [8,9], blend with other polymers [10,11], modification with polypyrrole [12] and interfacial graft copolymerization [13,14]. These modification approaches are indeed effective for reduction of vanadium crossover. However, since Nafion[®] is very expensive, cost seems to be still a major concern associated with these modified membranes. Besides Nafion[®], in the past decade many cost-effective and high performance hydrocarbon polymer membranes have been attempted as alternative for VRBs such as sulfonated poly(aryl ether ketone)s [15–22], sulfonated poly(aryl ether sulfone)s [23–25], branched sulfonated poly(fluorenyl ether ketone sulfone)s [26], sulfonated polyimides [27–30], sulfonated Diels Alder poly(phenylene) [31], poly(vinyl difluoride)-*g*-poly(styrene-

* Corresponding authors.

E-mail addresses: jhfang@sjtu.edu.cn (J. Fang), weiming@iccas.ac.cn (W.-M. Zhang).

4-sulfonic acid-co-maleic anhydride) [32], and various anion exchange polymer membranes [33–42]. Unlike Nafion[®], hydrocarbon polymer membranes generally exhibit low vanadium cation permeability when their ion exchange capacities (IECs) are controlled at an appropriate level. This is because they lack perfect ionic channels as observed in Nafion[®] to facilitate vanadium cation transport. For example, Sankir and coworkers reported that the sulfonated poly(aryl ether sulfone) membrane (BPSH 35) displayed one order of magnitude lower vanadium permeability but even higher proton conductivity than Nafion 212 [23]. Very recently Zhang and co-workers reported that the VRB assembled with a cross-linked anion exchange membranes derived from chloromethylated polysulfone and 4,4'-bipyridine exhibit very high energy efficiencies (88.3–81.8%) in the current density range of 80–140 mA cm⁻² which are superior to those (83.2–76.1%) assembled with Nafion 115 in the same current range owing to the high ionic conductivity and low vanadium crossover of the former [33]. The very low vanadium permeability of the anion exchange membranes is ascribed to the Donnan exclusion effect and the cross-linking network [33].

Because hydrocarbon polymers are generally less stable to oxidation than perfluorinated polymers, chemical stability in highly oxidative environment is an important concern to most hydrocarbon polymer membranes for use in VRBs (VO₂⁺ is highly oxidative in acidic solution). To achieve long-term durability of VRBs, it is very crucial to select polymers with highly stable backbones. Heterocyclic polymers, in particular, polybenzimidazoles (PBIs), are known for their excellent chemical stability to oxidation [43–45]. However, up to date, quite few publications on PBI-based separators are reported. Zhou et al. reported that the commercial PBI membrane showed only 2.9% weight loss after soaking testing in 1 M VO₂⁺ at room temperature for 120 days which is comparable to that of Nafion[®] [46]. The VBR assembled with the PBI membrane exhibited a substantially higher coulombic efficiency of up to 99% at current densities ranging from 20 mA cm⁻² to 80 mA cm⁻² due to very low vanadium cation permeability of the PBI membrane. Liao et al. reported that the benzimidazole groups-containing sulfonated poly(aryl ether ketone) membranes exhibit ultra-low vanadium ion diffusion due to the acid-base interaction (ionic cross-linking) and the exclusion effect between the positively-charged (protonated) benzimidazole groups and vanadium cations [15]. The VRBs assembled with their membranes exhibit little performance decay after 200 charge-discharge cycles.

Herein, for the first time we report on the preparation of covalently cross-linked sulfonated polybenzimidazole (CSOPBI) membranes and their VBR performance. The highly inert PBI backbones is expected to ensure excellent chemical stability to the highly oxidative electrolyte (VO₂⁺). The covalent cross-linking network in combination with Donnan exclusive effect resulting from the protonated imidazole groups and vanadium cations are favorable for prohibiting vanadium cation crossover, while the sulfonic acid groups are responsible for proton transport.

2. Experimental

2.1. Materials

4,4'-Dicarboxydiphenyl ether (DCDPE), 3,3'-Diaminobenzidine (DAB) and 5-aminoisophthalic acid (APTA) were purchased from Acros and used without further purification. Polyphosphoric acid (PPA), bisphenol A diglycidyl ether (BADGE) and dimethylsulfoxide (DMSO) were purchased from Sinopharm Chemical Reagent Co., Ltd. (SCRC). APTA was dried at 80 °C in vacuum for 10 h before use. DMSO was directly dried over 4A molecular sieves prior to use. Other materials were used as received.

2.2. Synthesis of polybenzimidazole copolymers

The synthetic procedures are described as follows using the copolybenzimidazole comprising DCDPE and APTA moieties at the molar ratio of 9:1 (the copolymer is denoted as OPBI-NH₂(9/1) as an example.

To a 250 mL dry three-neck flask were added 2.32 g (9.0 mmol) of DCDPE, 0.181 g of (1.0 mmol) APTA, 2.14 g (10.0 mmol) of 3,3'-diaminobenzidine (DAB) and 60 g of PPA under nitrogen flow. The reaction mixture was mechanically stirred and slowly heated to 150 °C and kept at this temperature for 2 h. The reaction temperature was further raised to 190 °C and maintained for another 20 h. While hot the resulting solution mixture was slowly poured into 300 g of ice water with stirring. The precipitated product was first washed with deionized water for three times and then soaked in 5 wt% sodium bicarbonate solution for 24 h. The solid was thoroughly washed with deionized water till pH neutral and dried in vacuum at 60 °C for 20 h.

The same procedures were followed to synthesize other polybenzimidazole copolymers comprising of DCDPE and APTA moieties at the molar ratio of 5:1, 4:1 and 3:1, respectively (the copolymers are denoted as OPBI-NH₂(5/1), OPBI-NH₂(4/1), OPBI-NH₂(3/1), respectively).

2.3. Post-sulfonation

To a 100 mL dry three-neck flask were added 2.0 g of a polybenzimidazole copolymer and 20 mL of fuming sulfuric acid (20% SO₃) under nitrogen flow. The mixture was mechanically stirred at room temperature for 0.5 h and then slowly heated to 100 °C and kept at this temperature for 12 h. After cooling to room temperature, the highly viscous solution mixture was slowly poured into 200 mL of ice water with stirring. The precipitate was collected by filtration, soaked in 5 wt % sodium bicarbonate solution for 24 h and finally washed with deionized water till pH neutral. The solid was dried in vacuum at 60 °C for 20 h. The resulting sulfonated polybenzimidazole copolymers are denoted as SOPBI-NH₂(x/y). Here, x/y refers to the molar ratio of DCDPE to APTA (9/1, 5/1, 4/1 and 3/1).

2.4. Membrane formation and proton exchange treatment

The sulfonated polybenzimidazoles were dissolved in DMSO to give 5 w/v% solutions. Then stoichiometric amount of the cross-linker BADGE was added to the solutions (the molar ratio of the BADGE to the APTA moiety of the sulfonated polybenzimidazoles was controlled at 1:1). The solution mixtures was filtered and subsequently cast onto clean glass plates and dried in an air oven at 80 °C for 8 h. The resulting membranes were peeled off from glass plates and further dried in vacuum at 120 °C for 10 h. They are denoted as CSOPBI-NH₂(x/y). Here, x/y refers to the same meaning as foregoing mentioned.

Proton exchange treatment was performed by immersing the membranes in 1.0 M H₂SO₄ solution at room temperature for 3 days. Then the membrane was thoroughly washed with deionized water until the rinsed water became pH neutral. Finally the membranes were dried at 120 °C for 10 h in vacuum.

2.5. Characterization of membranes

FT-IR spectra were recorded on a Perkin-Elmer Paragon 1000PC spectrometer. ¹H NMR spectra were recorded on a Varian Mercury Plus 400 MHz instrument. Thermogravimetric analysis (TGA) was performed in air with a TGA2050 instrument at a heating rate of 10 °C min⁻¹. Elemental analysis test was performed with a Vario EL Cube instrument (Elementar, Germany).

Ion exchange capacity (IEC) was measured by titration method. The dry membranes (0.2–0.3 g per sheet) were cut into small pieces and

soaked in a saturated sodium chloride solution at room temperature for three days. Then the sample pieces were either taken out and rinsed with deionized water three times (manner 1) or kept in the solution (manner 2). For method 1, the rinsed water was combined with the previous sodium chloride solution and then titrated with a 0.01 M sodium hydroxide solution using phenolphthalein as a pH indicator. For method 2, the mixture (membrane sheets+solution) was directly titrated with a 0.01 M sodium hydroxide solution using phenolphthalein as a pH indicator.

Water uptake (WU) measurements were carried out by immersing the dry membranes in their proton form (0.2–0.3 g per sheet) into deionized water at 40 °C for 5 h. Then the membranes were taken out, wiped with tissue paper, quickly weighed on a microbalance. WU was calculated from the following equation:

$$WU = (W_s - W_d) / W_d \times 100\% \quad (1)$$

where W_d and W_s refer to the weight of dry and wet membranes, respectively.

Acid sorption test was carried out by immersing the dry membranes in their proton form (0.2–0.3 g per sheet) into 50 mL of 2.0 mol L⁻¹ sulfuric acid at 40 °C for 48 h. During this process, both water and sulfuric acid were gradually absorbed in the membranes. Then the membranes were taken out, wiped with tissue paper, quickly weighed on a microbalance, and dried in a vacuum oven at 60 °C for 10 h to remove the absorbed water (sulfuric acid was remained in the membranes). The dried samples were quickly weighed on a microbalance. The total liquid uptake S_{total} (the sum of water and sulfuric acid) was calculated from Eq. (2):

$$S_{total} = (W - W_0) / W_0 \times 100\% \quad (2)$$

where W_0 and W refer to the weight of dry membranes before acid sorption test and the weight of the wet membranes prior to vacuum drying, respectively.

The fraction of sulfuric acid absorbed in the membranes (S_{acid}) was calculated from Eq. (3):

$$S_{acid} = (W_1 - W_0) / W_0 \times 100\% \quad (3)$$

where W_1 refers to the weight of dry membranes after acid sorption test and vacuum drying.

The fraction of water absorbed in the membranes (S_{water}) was calculated from Eq. (4):

$$S_{water} = S - S_{acid} \quad (4)$$

The in-plane swelling ratio (Δl) and the through-plane swelling ratio (Δt) of the membranes in 2.0 mol L⁻¹ sulfuric acid at 40 °C were calculated from Eqs. (5) and (6):

$$\Delta l = (l_s - l_d) / l_d \times 100\% \quad (5)$$

$$\Delta t = (t_s - t_d) / t_d \times 100\% \quad (6)$$

where l_d and t_d were the length and thickness of the dry membranes, respectively, while l_s and t_s referred to the length and thickness of the wet membranes.

The in-plane proton conductivity σ was measured using a four-point-probe cell by electrochemical impedance spectroscopy over the frequency range from 42 Hz to 5 MHz (3532-50 LCR, Hioki E. E. Corporation). The membranes in their proton form were mounted in a cell made of poly(tetrafluoroethylene) together with two pairs of platinum electrodes. The cell was immersed into distilled deionized water and the test was performed at room temperature. The ohmic resistance R was determined from the intercept of the impedance with the real axis. Proton conductivity was calculated from the following equation:

$$\sigma = D / (LBR) \quad (7)$$

where D was the distance between the two electrodes, L and B were the thickness and width of the membrane, respectively.

Tensile measurements were carried out with an Instron 4456 instrument under ambient atmosphere (room temperature, ~50% relative humidity) at a crosshead speed of 1 mm min⁻¹. For each kind of membrane, three sheets of samples were used for the measurements and the tensile stress (TS) and the elongation at break (EB) was estimated by the averaged values of the three samples.

Permeability of vanadium ions through cross-linked sulfonated polybenzimidazole membranes or Nafion117 was investigated according to the method described by Zhai et al. [47]. Before test, all the membranes were activated by immersing into deionized water for about 24 h. Then a sheet of membrane was exposed to a solution of 1 mol L⁻¹ VOSO₄ in 2 mol L⁻¹ sulfuric acid on one side and a solution of 1 mol L⁻¹ MgSO₄ in 2 mol L⁻¹ sulfuric acid on the other side. MgSO₄ was used to equalize the ionic strengths of the two solutions and to minimize the osmotic pressure effects. Area of the membrane exposed to the solution was 12.0 cm² and volume of solutions in both sides was 20 mL. The MgSO₄ solution was taken for UV-vis analysis at pre-determined intervals and concentration of vanadium ion in the solution was determined. The solution was returned to the test reservoir immediately after the test to minimize the change of test solution. Diffusion coefficients of the vanadium ions across the membranes in a vanadium redox flow battery were calculated based on the equation mentioned in Luo's work [10]. The concentration of vanadium ions in MgSO₄ solution side as a function of time is given according to the following equation:

$$V \frac{dC_t}{dt} = S \frac{P}{L} (C_0 - C_t) \quad (8)$$

where V is the volume of the solution in both sides; S is the area of the membrane exposed to the solution; P is the diffusion coefficient of vanadium ions; L is the thickness of the membrane; C_0 is the initial VO²⁺ concentration in VOSO₄ reservoir; C_t is the VO²⁺ concentration in MgSO₄ reservoir at time (t). Assumption is suggested that P is independent of concentration. In our experiments, C_t (less than 20 mM) is much lower than C_0 (1.0 M). According to Eq. (9), diffusion coefficient P can be given as Eq. (8):

$$P = \frac{VL}{SC_0} \frac{dC_t}{dt} \quad (9)$$

The ion diffusion selectivity of proton over vanadium cation (H/V) was measured in a diffusion cell by a previously reported method [48]. Before the test, the left cell was filled with 50 mL of 1.0 M VOSO₄ and 2.0 M H₂SO₄, and the right cell was filled with 50 mL of deionized water. Both sides of the solutions are stirred to avoid concentration polarization. The tests were stopped after a specific period of time (6–24 h) and the solution samples from the right cell were collected for further analysis. The proton concentrations were determined by automatic potentiometric titration (INESAZDJ-4B automatic titrator), and the concentrations of VO²⁺ were analyzed by ICP-OES (Perkin-Elmer Optima 8000). The H/V selectivity is defined by the following equation [48]:

$$H/V \text{ selectivity} = \frac{H^+ \text{ permeation rate}}{VO^{2+} \text{ permeation rate}} \quad (10)$$

2.6. VRB single cell test

The VRB used was assembled by sandwiching the membrane between two pieces of graphite carbon electrodes (thickness: 6 mm). The anodic electrolyte was 2.0 mol L⁻¹ V³⁺ in 2.0 mol L⁻¹ sulfuric acid solution and cathodic electrolyte was 2.0 mol L⁻¹ VO²⁺ in 2.0 mol L⁻¹ sulfuric acid solution respectively. Effective area of the membrane exposed to the solution was 12 cm² and volume of solutions in both sides was 10 mL. The recirculation rate of electrolyte was 10 mL min⁻¹ and the flow velocity was 0.38 cm s⁻¹ in the VRB cell. The

battery was first charged to 1.7 V with a current density of 40 mA cm^{-2} and then the open circuit voltage (OCV) was measured at room temperature. The OCV and charge/discharge tests were applied with Land CT2001A battery evaluation system at room temperature. The coulombic efficiency (CE), voltage efficiency (VE) and energy efficiency (EE) were calculated according to the following equations :

$$CE = (C_d / C_c) \times 100\% \quad (11)$$

$$VE = (V_d / V_c) \times 100\% \quad (12)$$

$$EE = CE \cdot VE \quad (13)$$

where C_d and C_c were discharge/charge capacity, V_d and V_c were discharge/charge average voltage.

The charge-discharge cycle test was performed by controlling the voltage limit at 1.7 V for charge and 0.8 V for discharge at a given current density (60 mA cm^{-2}) at $\sim 20^\circ\text{C}$. Other conditions such as the electrolyte concentration and volume for anode and cathode, electrolyte flow velocity and membrane effective area were exactly the same as those described above. The initial charge/discharge capacity is about 500 mA h, which is about state of charge (SOC) 3–97% in this work.

3. Results and discussion

3.1. Polymer synthesis and characterization

As shown in Scheme 1, a series of sulfonated polybenzimidazole copolymers with varied content of pendant amino groups were synthesized by two-step reactions. The purpose of introducing pendant amino groups to the polymer structure is to provide cross-linking sites for preparation of covalently cross-linked membranes as will be discussed in the following section. The first step reaction involves the condensation copolymerization of DCDPE, APTA and DAB in PPA at 190°C . The monomer molar ratio was controlled at DCDPE/APTA = 9/1, 5/1, 4/1 and 3/1, and the resulting polybenzimidazole copolymers are denoted as **OPBI-NH₂(9/1)**, **OPBI-NH₂(5/1)**, **OPBI-NH₂(4/1)** and **OPBI-NH₂(3/1)**, respectively. These copolymers further underwent post-sulfonation reaction in the second step using fuming sulfuric acid as the sulfonating reagent at 100°C to yield the sulfonated polybenzimidazole copolymers **SOPBI-NH₂(x/y)** (here, x/y refers to the monomer molar ratio of DCDPE to APTA). Fig. 1 shows the FT-IR spectra of the prepared sulfonated polybenzimidazole copolymers in their acid form. The extremely broad band around 3400 cm^{-1} is

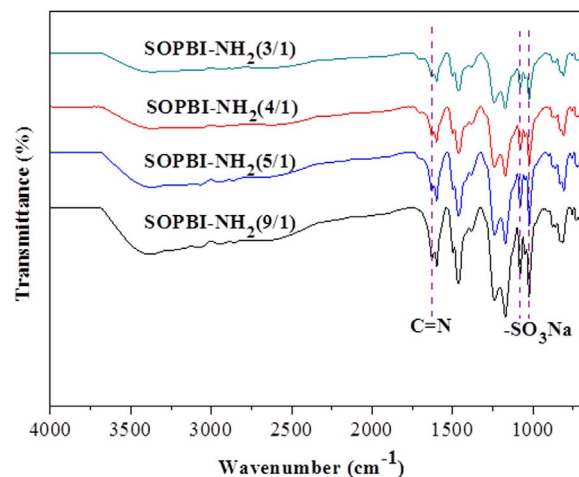
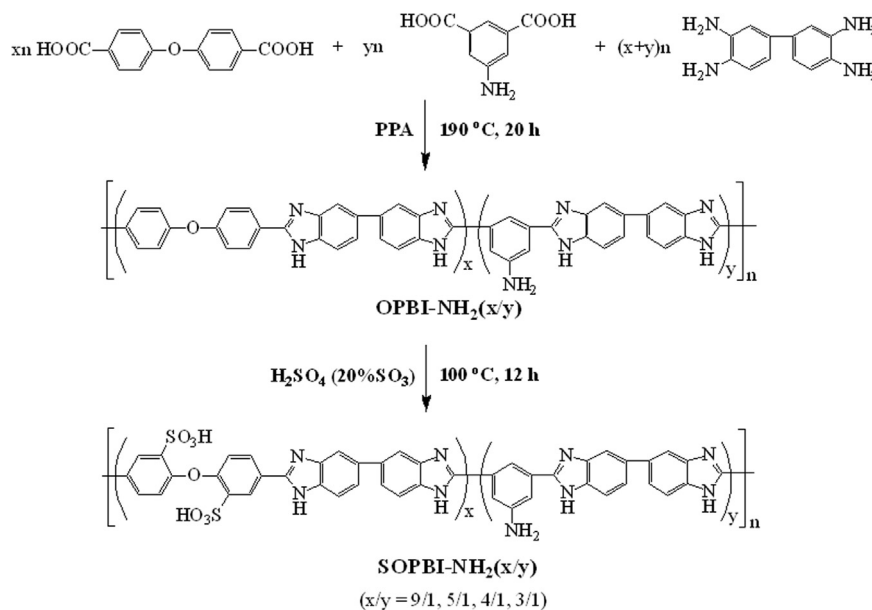


Fig. 1. FT-IR spectra of the prepared sulfonated polybenzimidazole copolymers in their acid form.

attributed to the stretch vibrations of both N-H (imidazole groups and $-\text{NH}_2$) and O-H (absorbed water and sulfonic acid groups). The characteristic absorption bands around 1628 cm^{-1} (C=N stretch) and 1462 cm^{-1} (in-plane deformation of imidazole rings) suggests the formation of imidazole rings [44,49]. The absorption bands around 1080 and 1024 cm^{-1} are assigned to asymmetric and symmetric stretch of the sulfonic acid groups [44,50], respectively, indicating that sulfonation has been successfully achieved.

It should be noted that the sulfonation reaction preferentially occurs on the DCDPE moiety because the two benzene rings of the DCDEP moiety are activated due to the presence of electron-donating bond (ether bond), while the benzene rings of the DAB and APTA moieties could hardly be sulfonated because they are highly deactivated due to the strong electron-withdrawing effect of the protonated imidazole rings and the protonated amino groups. For the APTA moiety, steric effect should be another reason for its low reactivity to sulfonation. Fig. 2 shows the ^1H NMR spectra of the synthesized **OPBI-NH₂(3/1)** and **SOPBI-NH₂(3/1)**. The peak around 8.75 ppm in the spectrum of the **SOPBI-NH₂(3/1)** is assigned to the protons adjacent to sulfonate groups, while such a peak is not observed in the spectrum of the **OPBI-NH₂(3/1)**.

The degree of sulfonation of the sulfonated polybenzimidazole



Scheme 1. Synthesis of polybenzimidazole copolymers with varied content of pendant amino groups.

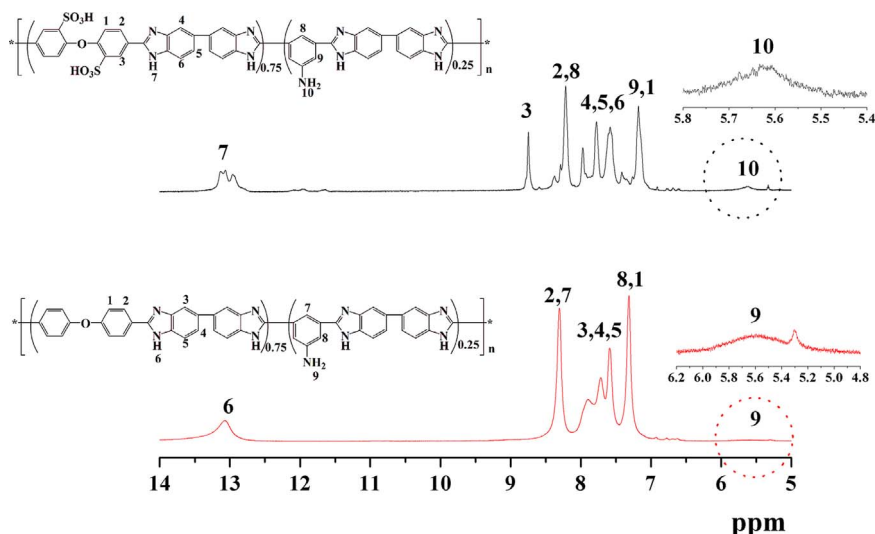


Fig. 2. ^1H NMR spectra of the $\text{OPBI-NH}_2(3/1)$ and $\text{SOPBI-NH}_2(3/1)$ in DMSO-d_6 .

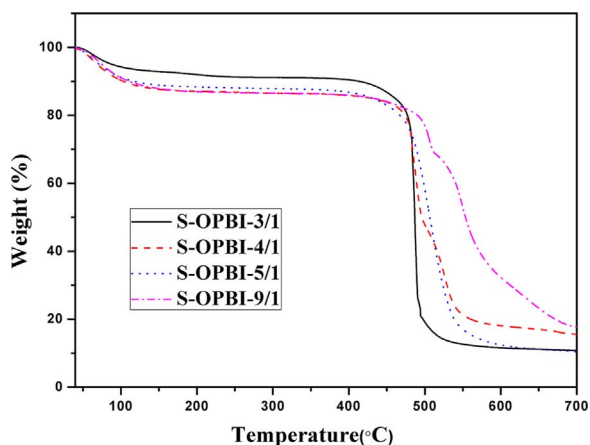


Fig. 3. TGA curves of the sulfonated polybenzimidazole copolymers in their sodium salt form.

copolymers in their sodium salt form was determined by elemental analysis. Since the sulfonated polybenzimidazole copolymers are highly hydrophilic, they readily absorb moisture from air. Therefore, the water content in samples should be included in chemical formulae for calculation when doing elemental analysis. The water content in samples was determined by TGA. As shown in Fig. 3, the first stage (from room temperature to ~ 150 °C) weight loss is assigned to evaporation of water absorbed in samples and the values are 18.5%,

15.2%, 15.5% and 15.4%, which correspond to 7.3, 5.5, 5.6 and 5.4 water molecules per repeat unit (averaged) for the $\text{SOPBI-NH}_2(9/1)$, $\text{SOPBI-NH}_2(5/1)$, $\text{SOPBI-NH}_2(4/1)$ and $\text{SOPBI-NH}_2(3/1)$, respectively. The second stage weight loss starting from ~ 400 °C is due to decomposition of sodium sulfonate groups and polymer backbone. The elemental analysis results are shown in Table 1. It can be seen that the DCDPE moiety is approximately disulfonated for all the sulfonated copolymers.

The prepared sulfonated polybenzimidazole copolymers in their sodium salt form are soluble in common aprotic solvents such as DMSO, *N,N*-dimethylacetamide (DMAc) and 1-methylpyrrolidone (NMP) upon slight heating. However, in their acid form they became insoluble in these solvents owing to the ionic cross-linking resulting from the interaction between the acidic groups (sulfonate groups) and the basic groups (benzimidazole groups and primary amino groups).

3.2. Covalent cross-linking and mechanical properties

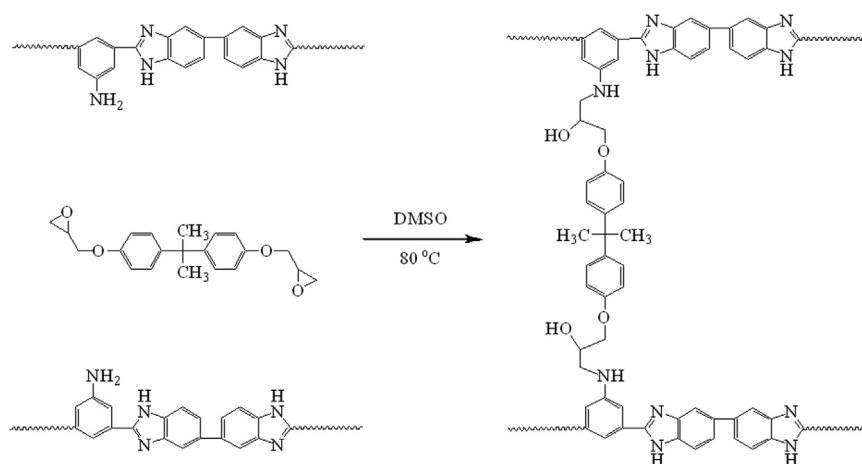
The pendant amino groups of the sulfonated polybenzimidazole copolymers were used as the cross-linking groups and the epoxy resin (BADGE) was used as the cross-linker. Covalent cross-linking occurred during the process of solution cast at 80 °C and the resulting cross-linked membranes are denoted as $\text{CSOPBI-NH}_2(x/y)$ (here, x/y refers to the monomer molar ratio of DCDPE to APTA). The formation of covalent cross-linking was confirmed by the fact that the prepared $\text{CSOPBI-NH}_2(x/y)$ membranes became completely insoluble in DMSO on heating, whereas the $\text{SOPBI-NH}_2(x/y)$ membranes pre-

Table 1

Elemental analysis results of the synthesized sulfonated polybenzimidazole copolymers in their sodium salt form.

Polymer	Formula ^a	C (%)		H (%)		N (%)		S (%)	
		Cal.	Found	Cal.	Found	Cal.	Found	Cal.	Found
$\text{SOPBI-NH}_2(9/1)$	$\text{C}_{25.4}\text{H}_{13.9}\text{N}_{4.1}\text{S}_{1.8}\text{O}_{6.3}\text{Na}_{1.8}\cdot(\text{H}_2\text{O})_{7.3}$	43.14	44.56	4.17	3.84	8.12	8.25	8.15	7.72
$\text{SOPBI-NH}_2(5/1)$	$\text{C}_{25}\text{H}_{13.8}\text{N}_{4.2}\text{S}_{1.67}\text{O}_{5.8}\text{Na}_{1.67}\cdot(\text{H}_2\text{O})_{5.5}$	45.72	49.95	3.78	4.51	8.89	9.76	8.12	5.83
$\text{SOPBI-NH}_2(4/1)$	$\text{C}_{24.8}\text{H}_{13.8}\text{N}_{4.2}\text{S}_{1.6}\text{O}_{5.6}\text{Na}_{1.6}\cdot(\text{H}_2\text{O})_{5.6}$	45.88	45.03	3.85	4.44	9.07	8.38	7.89	7.21
$\text{SOPBI-NH}_2(3/1)$	$\text{C}_{24.5}\text{H}_{13.8}\text{N}_{4.3}\text{S}_{1.5}\text{O}_{5.3}\text{Na}_{1.5}\cdot(\text{H}_2\text{O})_{5.4}$	46.60	46.68	3.89	4.22	9.43	9.30	7.61	7.62

^a The copolymer formulae are obtained by assuming that the DCDPE moiety is disulfonated, while the absorbed water in the samples is estimated from TGA curves.



Scheme 2. Covalent cross-linking reaction.

pared in the absence of BADGE were well soluble in DMSO. The cross-linking reaction is depicted in Scheme 2.

The tensile stress (TS) and the elongation at break (EB) values of the *non*-cross-linked and the cross-linked membranes are shown in Table 2. It can be seen that the covalent cross-linking caused great increases in TS but large decreases in EB. For example, the TS of the **SOPBI-NH₂(9/1)** increased from 48 MPa to 85 MPa after cross-linking, while the EB decreased from 73% to 16%. The decreased EB is due to the presence of the cross-linking network in the cross-linked membranes which restricts the displacement of polymer chains. It should be noted that the EB values of all the covalently cross-linked membranes are larger than 5% indicating that they possess reasonable toughness despite the occurrence of covalent cross-linking and ionic cross-linking. From this table, it can also be seen that the TS values of the covalently cross-linked membranes (85–98 MPa) are approximately three times higher than that of Nafion117 (26 MPa) [51].

3.3. IEC, acid sorption, swelling ratio and proton conductivity

IEC is one of the key properties of an ionomer. In this study, the determination of IEC was performed via two manners. For manner 1, the membrane samples in their proton form were removed from the sodium chloride solutions prior to titration with a sodium hydroxide solution. As shown in Table 3, for all the *non*-cross-linked and cross-linked polybenzimidazole membranes the IEC values obtained by this manner are extremely low ($\sim 0.2 \text{ meq g}^{-1}$, approach to experimental error). This is because of the ionic cross-linking resulting from the acid-base interaction between sulfonic acid groups and imidazole rings of the polybenzimidazole membranes. The protons of sulfonate groups were so tightly bonded with the basic benzimidazole groups that they could be hardly exchanged with sodium cations. In contrast, for

Table 2

Tensile strength (TS) and elongation break (EB) of the *non*-cross-linked and the covalently cross-linked sulfonated polybenzimidazole membranes.

Membrane	Cross-linking	TS (MPa)	EB (%)	Ref.
SOPBI-NH₂(9/1)	No	48 ± 5.3	73 ± 9.8	This study
SOPBI-NH₂(5/1)	No	65 ± 2.5	86 ± 9.3	This study
SOPBI-NH₂(4/1)	No	50 ± 2.0	71 ± 11	This study
SOPBI-NH₂(3/1)	No	40 ± 5.0	53 ± 8.2	This study
CSOPBI-NH₂(9/1)	Yes	85 ± 0.7	16 ± 5.5	This study
CSOPBI-NH₂(5/1)	Yes	98 ± 3.6	6.3 ± 1.6	This study
CSOPBI-NH₂(4/1)	Yes	91 ± 2.3	5.5 ± 2.8	This study
CSOPBI-NH₂(3/1)	Yes	86 ± 1.5	5.5 ± 1.9	This study
Nafion 117	No	27	NA	50

NA: not available from literature.

manner 2, the membrane samples in their proton form were kept in the sodium chloride solutions during the process of titration. The IEC values obtained by manner 2 are in the range of $2.91\text{--}3.41 \text{ meq g}^{-1}$ for the *non*-cross-linked polybenzimidazole membranes and $2.61\text{--}3.15 \text{ meq g}^{-1}$ for the covalently cross-linked membranes which correspond to approximately disulfonation per DCDPE unit. This is consistent with the elemental analysis results as foregoing discussed. The basicity of sodium hydroxide is much stronger than that of benzimidazole groups and thus the protons bonded with benzimidazole groups can be dissociated and neutralized with hydroxide anions. The covalently cross-linked membranes exhibit slightly lower IEC than the corresponding *non*-cross-linked membranes because the cross-linker (BADGE) doesn't contain any ionic groups.

The water uptakes (WU) of the polybenzimidazole membranes measured in distilled ionized water at 40 °C are shown in Table 3. For the *non*-cross-linked polybenzimidazole membranes, the WU is in the order: **SOPBI-NH₂(9/1)** > **SOPBI-NH₂(5/1)** > **SOPBI-NH₂(4/1)** > **SOPBI-NH₂(3/1)**, which is consistent with the order of their IEC values (manner 2). For the covalently cross-linked polybenzimidazole membranes, a similar trend is observed. However, it should be noted that the WU values of the cross-linked membranes are only about half of those of the corresponding *non*-cross-linked membranes. The **CSOPBI-NH₂(9/1)** having the highest IEC (3.15 meq g^{-1} , manner 2) among the covalently cross-linked membranes exhibited much lower WU than the **SOPBI-NH₂(3/1)** having the lowest IEC (2.91 meq g^{-1} , manner 2) among the *non*-cross-linked membranes (WU: 47.4 w/w% vs. 75.6 w/w%). This indicates that the covalent cross-linking is very effective for suppression of membrane swelling.

Since the electrolyte used in a VRB system is vanadium salt dissolved in aqueous sulfuric acid and the free acid concentration in this study is 2.0 mol L^{-1} , the sorption and swelling behaviors of the sulfonated polybenzimidazole membranes in 2.0 mol L^{-1} sulfuric acid solution at 40 °C were investigated and the results are listed in Table 3. For comparison purpose, the sorption and swelling behaviors of Nafion117 were also measured. The total liquid uptake (S_{total}) is the sum of sulfuric acid (S_{acid}) and water (S_{water}) absorbed in the membranes. For the *non*-cross-linked membranes, the S_{total} , S_{acid} and S_{water} moderately decrease in the order: **SOPBI-NH₂(9/1)**, **SOPBI-NH₂(5/1)**, **SOPBI-NH₂(4/1)** and **SOPBI-NH₂(3/1)**, which is consistent with the trend of their WU. Moreover, for all the membranes the S_{water} is much larger than the S_{acid} indicating that water sorption is the predominant factor during the process of sulfuric acid sorption test. This is because of the low concentration of sulfuric acid solution (2 mol L^{-1}) employed for the sorption test.

For the covalently cross-linked polybenzimidazole membranes, the S_{total} and the S_{water} are in the range of 39.8–52.6 w/w% and 28.8–37.3

Table 3

Ion exchange capacity (IEC), water uptake (WU), liquid uptake and swelling ratio (SR) in 2 mol L⁻¹ sulfuric acid and proton conductivity (σ , in water) of the sulfonated polybenzimidazole membranes and Nafion 117 in their proton form.

Membrane	IEC (meq g ⁻¹)		WU ^c (w/w%)	Liquid Uptake ^d (w/w%)			SR ^d (%)		σ^f S cm ⁻¹
	Manner 1 ^a	Manner 2 ^b		S _{total}	S _{acid}	S _{water}	Δl^e	Δt^e	
SOPBI-NH ₂ (9/1)	0.24	3.41 (3.36)	98.2	85.0	11.1	73.9	15	21	0.035
SOPBI-NH ₂ (5/1)	0.26	3.18 (3.20)	91.0	79.7	6.80	72.7	14	20	0.028
SOPBI-NH ₂ (4/1)	0.18	3.10 (3.12)	84.7	75.7	5.30	70.4	13	17	0.024
SOPBI-NH ₂ (3/1)	0.21	2.91 (3.00)	75.6	63.4	3.50	59.9	10	13	0.019
CSOPBI-NH ₂ (9/1)	0.12	3.15 (3.16)	47.4	52.6	15.3	37.3	6.6	10	0.032
CSOPBI-NH ₂ (5/1)	0.11	2.87 (2.88)	40.0	50.5	14.3	36.2	6.1	9.7	0.025
CSOPBI-NH ₂ (4/1)	0.090	2.76 (2.76)	38.5	43.2	13.3	29.9	4.3	9.1	0.021
CSOPBI-NH ₂ (3/1)	0.12	2.61 (2.56)	36.8	39.8	11.0	28.8	3.8	6.8	0.012
Nafion117	0.91	0.91	NM	19.4	1.7	17.7	5.1	7.6	0.070

NM: not measured.

^a Membrane samples were removed from saturated sodium chloride solution before titration.

^b Membrane samples were kept in saturated sodium chloride solution during the process of titration. The data in parenthesis refer to the theoretical values calculated on the basis of disulfonation per DCDPE moiety.

^c Measured in distilled deionized water at 40 °C for 5 h.

^d Measured by soaking membranes in 2 mol L⁻¹ sulfuric acid at 40 °C for 5 h.

^e Δl : in-plane swelling ratio; Δt : through-plane swelling ratio.

^f Measured in deionized water at room temperature.

w/w%, respectively, which are significantly lower than those (63.4–85.0 w/w% and 62.2–73.9 w/w%) of the corresponding *non*-cross-linked membranes. This indicates that membrane swelling in aqueous sulfuric acid solution is also significantly suppressed due to the covalent cross-linking. In addition, both the S_{total} and the S_{water} slightly decrease in the order: CSOPBI-NH₂(9/1), CSOPBI-NH₂(5/1), CSOPBI-NH₂(4/1) and CSOPBI-NH₂(3/1), which is similar to the case of the *non*-cross-linked membranes. However, the S_{acid} values of the cross-linked membranes are higher than the corresponding *non*-cross-linked ones. At present, it is difficult to give a reasonable explanation. More work is needed to identify the acid sorption mechanism of the covalently cross-linked membranes.

For all the membranes, the in-plane swelling ratio (Δl) is slightly lower than the through-plane swelling ratio (Δt). The covalently cross-linked polybenzimidazole membranes exhibit rather low Δl (3.8–6.6%) and Δt (6.8–10%) which are only about half of those of the corresponding *non*-cross-linked membranes. The CSOPBI-NH₂(3/1) exhibited the lowest Δl and Δt because of its highest covalent cross-linking density as well as the lowest IEC.

It is interesting to compare the liquid uptakes and swelling ratios of the sulfonated polybenzimidazole membranes with those of Nafion 117. As shown in Table 3, unlike the polybenzimidazole membranes Nafion 117 hardly absorbed sulfuric acid (S_{acid} = 1.7 w/w%) probably because of its rather low affinity to sulfuric acid. The *non*-cross-linked polybenzimidazole membranes displayed much higher swelling ratios (Δl =10–15%, Δt =13–21%) than Nafion 117 (Δl =5.1%, Δt =7.6%) because of the much higher IECs of the former. This is an obvious disadvantage of the *non*-cross-linked polybenzimidazole membranes. Fortunately, however, all the covalently cross-linked membranes exhibit rather low swelling ratios which are close to that of Nafion 117. This clearly indicates that the covalent cross-linking is effective and essential.

The proton conductivities of the *non*-cross-linked polybenzimidazole membranes in deionized water at ambient temperature are in the range of 0.019–0.035 S cm⁻¹ and the membranes with higher IECs (manner 2) tend to have higher proton conductivities. The covalently cross-linked polybenzimidazole membranes exhibit slightly lower proton conductivities than the corresponding *non*-cross-linked membranes under the same conditions. Despite their much higher IECs, the sulfonated polybenzimidazole membranes exhibit significantly lower proton conductivities than Nafion 117. This is because the sulfonic acid protons in the polybenzimidazole membranes are bonded to imidazole rings (ionic cross-linking) which is unfavorable for proton

transport.

3.4. Vanadium cation permeability and ion diffusion selectivity

Crossovers of vanadium cations through the proton exchange membrane will cause serious self-discharge of the battery and result in low energy efficiency of the VRB, which will limit the application of membranes in VRB. It is highly desirable to develop proton exchange membranes with excellent inhibitory effect on vanadium cations crossover.

Because the *non*-cross-linked polybenzimidazole membranes highly swelled in aqueous sulfuric acid solution, they are expected to be unfavorable for VRB applications. Hence, their VRB performances were not examined. The permeabilities of vanadium cations across the covalently cross-linked membranes (CSOPBI-NH₂(9/1), CSOPBI-NH₂(4/1) and CSOPBI-NH₂(3/1)) and Nafion 117 were determined by using a dialysis cell as described by Zhai et al. [47]. VO²⁺ was selected for the dialysis test because it is relatively stable in comparison with other valence number vanadium cations. The variation of VO²⁺ concentration (C_t) in permeate side (MgSO₄ solution) as a function of time is illustrated in Fig. 4. From this figure in combination with Eq. (7), the diffusion coefficients (P) can be readily calculated. The diffusion coefficient of VO²⁺ across Nafion 117 obtained in this study

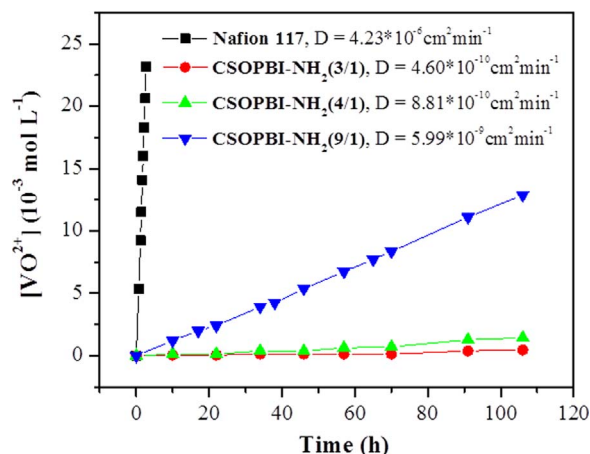


Fig. 4. Variation of VO²⁺ concentration in permeate side with different membranes as a function of time. The diffusion coefficients of VO²⁺ are obtained from the slope of the plots.

is $4.23 \times 10^{-6} \text{ cm}^2 \text{ min}^{-1}$ which is close to the values reported by other groups ($3 \times 10^{-6} \text{ cm}^2 \text{ min}^{-1}$ [52], $3.655 \times 10^{-6} \text{ cm}^2 \text{ min}^{-1}$ [14] and $4.096 \times 10^{-6} \text{ cm}^2 \text{ min}^{-1}$ [53]). For the covalently cross-linked polybenzimidazole membranes of this study, the VO^{2+} diffusion coefficients are $5.99 \times 10^{-9} \text{ cm}^2 \text{ min}^{-1}$, $8.81 \times 10^{-10} \text{ cm}^2 \text{ min}^{-1}$ and $4.60 \times 10^{-10} \text{ cm}^2 \text{ min}^{-1}$ for the **CSOPBI-NH₂(9/1)**, **CSOPBI-NH₂(4/1)** and **CSOPBI-NH₂(3/1)**, respectively, which are 3–4 orders of magnitude lower than that of Nafion 117 indicating excellent vanadium cation inhibition property of the former. This is mainly attributed to both the low membrane swelling ratios resulting from the covalent cross-linking and the Donnan exclusion effect resulting from the protonated imidazolium groups (positively charged) and VO^{2+} of the **CSOPBI-NH₂(x/y)** membranes. Among the covalently cross-linked membranes, the one with higher content of APTA unit tends to have lower VO^{2+} diffusion coefficient due to its higher covalent cross-linking density. The **CSOPBI-NH₂(3/1)** membrane displayed the lowest VO^{2+} permeability because of its highest covalent cross-linking density.

Besides vanadium permeability, proton/vanadium diffusion selectivity (H/V) is another important parameter for characterization of separator performance. As foregoing mentioned, since VO^{2+} is relatively stable in comparison with other valence number vanadium cations, the permeability ratio of protons to VO^{2+} cations was measured to characterize the separators performance and the data are shown in Fig. 5. The selectivity values of the **CSOPBI-NH₂(x/y)** membranes are about 6–30 times larger than that of Nafion117 indicating much better performances of the former. Among the **CSOPBI-NH₂(x/y)** membranes, the selectivity is in the order: **CSOPBI-NH₂(3/1)** > **CSOPBI-NH₂(4/1)** > **CSOPBI-NH₂(9/1)**. This indicates that the selectivity is mainly determined by the covalent cross-linking density and the membranes with higher cross-linking density tend to have higher selectivity. This is likely because higher cross-linking density results in lower swelling ratio and thus higher ionic selectivity.

3.5. VRB performance

The charge-discharge curves of the VRBs assembled with the covalently cross-linked polybenzimidazole membranes at different current densities (20, 40, 60 and 80 mA cm^{-2}) at $\sim 10^\circ\text{C}$ are shown in Fig. 6. The voltage limit was controlled at 1.7 V for charge and 0.8 V for discharge. It can be seen that the discharge capacity is in the order: **CSOPBI-NH₂(9/1)** > **CSOPBI-NH₂(4/1)** > **CSOPBI-NH₂(3/1)** which is consistent with the order of proton conductivity. At low current density (20 mA cm^{-2}), the difference in discharge capacity was rather small. However, at high current densities the capacity difference became significantly larger. This is likely because at high current densities the effect of ionic conductivity on discharge capacity became more important.

The coulombic efficiency (CE), voltage efficiency (VE) and energy efficiency (EE) values of the VRBs assembled with the covalently cross-linked polybenzimidazole membranes and Nafion 117 at different

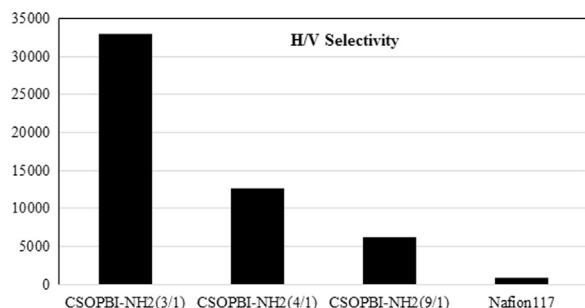


Fig. 5. Comparison of ion diffusion selectivity (H/V) of the cross-linked sulfonated polybenzimidazole membranes and Nafion117.

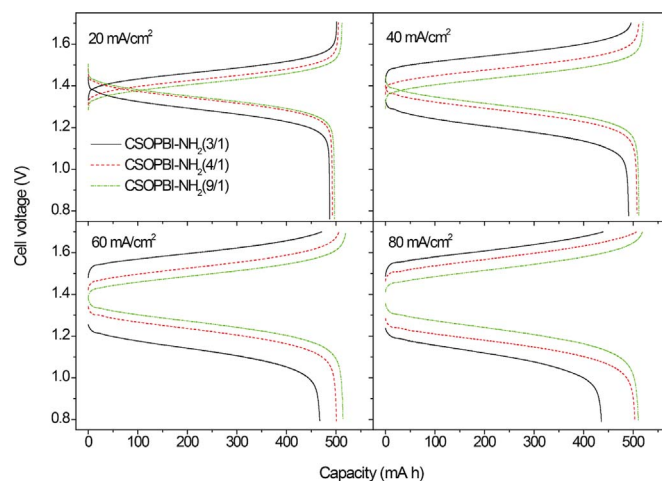


Fig. 6. Charge-discharge curves of the VRBs assembled with the covalently cross-linked polybenzimidazole membranes at different current densities at $\sim 10^\circ\text{C}$.

current density and an averaged ambient temperature of 10°C are shown in Fig. 7. For all the membranes the CE tends to increase with increasing current density and this effect is more significant at low current densities. At high current densities ($> 60 \text{ mA cm}^{-2}$), the CE values approach to nearly 100% for the VRBs assembled with the covalently cross-linked polybenzimidazole membranes and 93% for the one assembled with Nafion 117. This is because CE is closely related to vanadium cations crossover, and the more vanadium cations permeated through the membrane, the lower CE. At higher current densities the charge/discharge time became shorter and thus the impact of vanadium cations crossover was weakened. For the covalently cross-linked polybenzimidazole membranes with higher content of APTA unit, the corresponding cells exhibited higher CE due to their lower vanadium cations permeability resulting from their higher covalent cross-linking density. It is worth noting that the CE values of the VRBs assembled with the covalently cross-linked polybenzimidazole membranes are much higher than the one assembled with Nafion 117 especially at low current densities. For example, the cell assembled with the **CSOPBI-NH₂(9/1)** membrane displayed a CE value of 93% at 10 mA cm^{-2} , whereas the one assembled with Nafion 117 exhibited a CE value of only 72.5% at the same current density. This just coincides with the vanadium ions permeability test result as foregoing discussed. Unlike CE, the VE values of the VRBs assembled with the covalently cross-linked polybenzimidazole membranes are significantly lower than that of the one assembled with Nafion 117 especially at high current densities. Moreover, among the VRBs assembled with the **CSOPBI-NH₂(x/y)** membranes, VE is lower for the membrane with higher content of APTA unit. VE is a physical parameter related to cell inner resistance, and the higher resistance (lower ionic conductivity), the lower VE. As foregoing discussed, the proton conductivity is in the order: Nafion 117 > **CSOPBI-NH₂(9/1)** > **CSOPBI-NH₂(4/1)** > **CSOPBI-NH₂(3/1)**. The inner resistance values of the batteries are in a reverse order of these membranes in case of similar membrane thickness. In this study, although Nafion 117 is much thicker ($178 \mu\text{m}$) than the **CSOPBI-NH₂(x/y)** membranes ($50\text{--}60 \mu\text{m}$), the former still exhibited higher VE indicating that the inner resistance of the VRB cell assembled with Nafion 117 is lower than that of the cells assembled with the **CSOPBI-NH₂(x/y)** membranes. This should be attributed to the higher ionic (protonic and vanadium cations) conductivity of Nafion 117. Energy efficiency (EE) is the product of CE and VE. At low current densities ($\leq 20 \text{ mA cm}^{-2}$), the VRBs assembled with the **CSOPBI-NH₂(4/1)** and **CSOPBI-NH₂(9/1)** membranes showed high EE values of $\sim 90\%$ which are much higher than those (72.5% at 10 mA cm^{-2} , 81% at 20 mA cm^{-2}) of the one assembled with Nafion 117. This is because at low current densities all the VRB cells exhibited

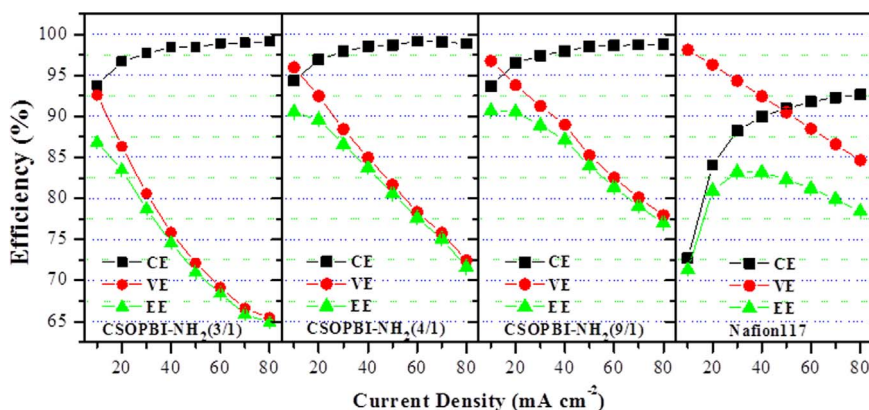


Fig. 7. Variation of efficiencies of VRB single cells assembled with different membranes at $-10\text{ }^{\circ}\text{C}$ as a function of current density.

high VE ($>92.5\%$) and CE became the dominant factor. In contrast, at high current densities ($>60\text{ mA cm}^{-2}$), the cells assembled with the **CSOPBI-NH₂(x/y)** membranes exhibited lower EE than the one assembled with Nafion 117 because in this case VE became a dominant factor. From this figure, it can also be seen that the cell assembled with the **CSOPBI-NH₂(9/1)** displayed the highest EE due to its highest VE among the **CSOPBI-NH₂(x/y)**-based VRBs.

The self-discharge rates of the VRBs were evaluated by the variation of open circuit voltage (OCV) as a function of time. As shown in Fig. 8, the OCV of the VRB assembled with Nafion117 membrane decreased rapidly after about 15 h, which is slightly longer than that reported in literature (11 h [10], 14 h [11]). In contrast, all the VRBs assembled with the **CSOPBI-NH₂(x/y)** membranes displayed significantly longer voltage maintaining time (lower self-discharge rate). The VRB assembled with the **CSOPBI-NH₂(3/1)** membrane exhibited the lowest self-discharge rate. Its OCV could be maintained above 1.4 V for 35 h which is more than twice as long as that of the one assembled with Nafion 117. This is attributed to the much lower vanadium cations permeability of the **CSOPBI-NH₂(x/y)** membranes than that of Nafion 117 as foregoing discussed. From this figure, it can also be seen that among the VRBs assembled with the **CSOPBI-NH₂(x/y)** membranes the self-discharge rate decreases with increasing the covalent cross-linking density which is also consistent with the vanadium cations permeability test results. In addition, the initial stage voltage decay (prior to voltage drastic dropping) rate is obviously lower for the VRBs assembled with the **CSOPBI-NH₂(x/y)** membranes than for the one assembled with Nafion 117 membrane. This is likely due to the better ionic selectivity of **CSOPBI-NH₂(x/y)** membranes, which redounds to keep high OCV. Such a phenomenon has been observed by many other groups [15,17,18,20].

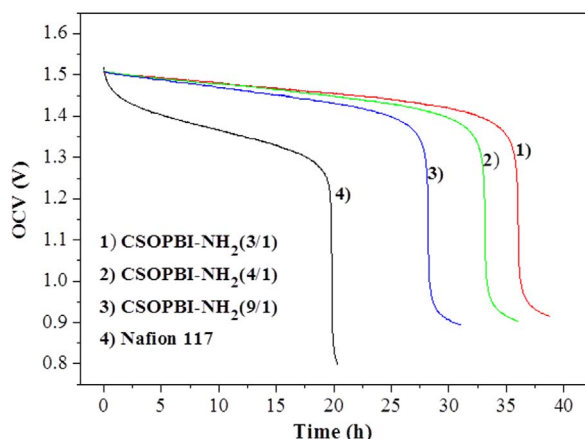


Fig. 8. Comparison of self-discharge behaviors of the VRB single cells assembled with the **CSOPBI-NH₂(9/1)**, **CSOPBI-NH₂(4/1)**, **CSOPBI-NH₂(3/1)** and Nafion 117.

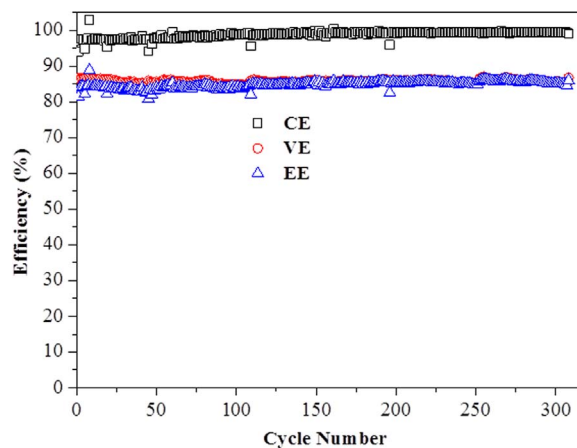


Fig. 9. The charge-discharge cycle performance of the VRB single cell assembled with the **CSOPBI-NH₂(9/1)** at a current density of 60 mA cm^{-2} at $-20\text{ }^{\circ}\text{C}$.

The durability test using the VRB single cell assembled with the **CSOPBI-NH₂(9/1)** membrane as an example was performed by charge-discharge cycling at a current density of 60 mA cm^{-2} at $-20\text{ }^{\circ}\text{C}$ and a preliminary result is shown in Fig. 9. The VRB did not exhibit any decay trend in cell performance after 300 charge-discharge cycles indicating good chemical stability of the **CSOPBI-NH₂(9/1)** membrane under the VRB operation conditions.

To further evaluate the chemical stability of the **CSOPBI-NH₂(x/y)** membranes, aging test was performed with **CSOPBI-NH₂(9/1)** and **CSOPBI-NH₂(5/1)** by soaking them in aqueous solution containing $1.4\text{ mol L}^{-1}\text{ VO}_2^+$ and 2 mol L^{-1} sulfuric acid at room temperature for one month. Then the membranes were taken out, thoroughly washed with deionized water, and finally dried in vacuum. The tensile properties of the pristine membranes and the membranes after the aging test were measured and the results are listed in Table 4. It is clear that for both membranes no significant reduction in tensile strength was observed (the difference is within experimental errors). This indicates that no significant polymer degradation occurred during the period of aging test. The excellent chemical stability of the membranes

Table 4
Comparison of tensile properties of the cross-linked sulfonated polybenzimidazole membranes after aging test (membranes were soaked in aqueous solution containing $1.4\text{ mol L}^{-1}\text{ VO}_2^+$ and 2 mol L^{-1} sulfuric acid at room temperature for one month).

Membrane	Stress (MPa)		Elongation at Break (%)	
	Before aging	After aging	Before aging	After aging
CSOPBI-NH₂(9/1)	85 ± 0.7	80 ± 4.9	16 ± 5.5	10 ± 1.0
CSOPBI-NH₂(5/1)	98 ± 3.6	103 ± 2.4	6.3 ± 1.6	5.1 ± 1.3

is likely ascribed to the highly stable heterocyclic main chains.

4. Conclusions

A series of covalently cross-linked sulfonated polybenzimidazole membranes (**CSOPBI-NH₂(x/y)**) with high IECs (2.61–3.15 meq g⁻¹) have been successfully prepared and their potential applications as novel separators in VRBs have been examined. The **CSOPBI-NH₂(x/y)** membranes exhibited 3–4 orders of magnitude lower vanadium cation permeability than Nafion117 because of the Donnan exclusion effect resulting from the protonated imidazolium groups (positively charged) and VO²⁺ as well as the covalent cross-linking, meanwhile the ion diffusion selectivity (H/V) values of the **CSOPBI-NH₂(x/y)** membranes are 6–30 times larger than that of Nafion117. The VRBs assembled with the **CSOPBI-NH₂(x/y)** membranes displayed significantly higher columbic efficiency and lower self-discharge rate than that assembled with Nafion 117 due to the much lower vanadium cation crossover of the former. The VRB assembled with the **CSOPBI-NH₂(9/1)** showed a high energy efficiency (~85%) at a current density of 60 mA cm⁻² at ~20 °C and little decay was observed after 300 cycles test making it promising candidate as high performance separator for VRB applications.

Acknowledgments

This study was supported by the National Basic Research Program of China (Grant no. 2014CB643600), the Shanghai Municipal Natural Science Foundation (Grant no. 13ZR1420200), the Special Fund of Shanghai Qingpu District-Shanghai Jiao Tong University Co-operation Program, and the GE (China) Research and Development Center Co., Ltd.

References

- [1] E. Sum, M. Skyllas-Kazacos, A study of the V(II)/V(III) redox couple for redox flow cell applications, *J. Power Sources* 15 (1985) 179–190.
- [2] E. Sum, M. Rychcik, M. Skyllas-Kazacos, Investigation of the V(V)/V(IV) system for use in the positive half-cell of a redox battery, *J. Power Sources* 16 (1985) 85–95.
- [3] A. Shibata, K. Sato, Development of vanadium redox flow battery for electricity storage, *Power Eng. J.* 13 (1999) 130–135.
- [4] W.Y. Hsu, T.D. Gierke, Elastic theory for ionic clustering in perfluorinated ionomers, *Macromolecules* 15 (1982) 101–105.
- [5] W.Y. Hsu, T.D. Gierke, Ion transport and clustering in nafion perfluorinated membranes, *J. Membr. Sci.* 13 (1983) 307–326.
- [6] C.-H. Lin, M.-C. Yang, H.-J. Wei, Amino-silica modified Nafion membrane for vanadium redox flow battery, *J. Power Sources* 282 (2015) 562–571.
- [7] J. Kim, J.-D. Jeon, S.-Y. Kwak, Nafion-based composite membrane with a permselective layered silicate layer for vanadium redox flow battery, *Electrochem. Commun.* 38 (2014) 68–70.
- [8] X. Teng, J. Dai, J. Su, Y. Zhu, H. Liu, Z. Song, A high performance polytetrafluoroethene/Nafion composite membrane for vanadium redox flow battery application, *J. Power Sources* 240 (2013) 131–139.
- [9] X. Teng, J. Dai, F. Bi, G. Yin, Ultra-thin polytetrafluoroethene/Nafion/silica composite membrane with high performance for vanadium redox flow battery, *J. Power Sources* 272 (2014) 113–120.
- [10] Z. Mai, H. Zhang, X. Li, S. Xiao, H. Zhang, Nafion/polyvinylidene fluoride blend membranes with improved ion selectivity for vanadium redox flow battery application, *J. Power Sources* 196 (2011) 5737–5741.
- [11] B. Schwenzer, S. Kim, M. Vijayakumar, Z. Yang, J. Liu, Correlation of structural differences between Nafion/polyaniline and Nafion/polypyrrole composite membranes and observed transport properties, *J. Membr. Sci.* 372 (2011) 11–19.
- [12] J. Zeng, C. Jiang, Y. Wang, J. Chen, S. Zhu, B. Zhao, R. Wang, Studies on polypyrrole modified nafion membrane for vanadium redox flow battery, *Electrochem. Commun.* 10 (2008) 372–375.
- [13] J. Ma, S. Wang, J. Peng, J. Yuan, C. Yu, J. Li, X. Ju, M. Zhai, Covalently incorporating a cationic charged layer onto Nafion membrane by radiation-induced graft copolymerization to reduce vanadium ion crossover, *Eur. Polym. J.* 49 (2013) 1832–1840.
- [14] Q. Luo, H. Zhang, J. Chen, P. Qian, Y. Zhai, Modification of Nafion membrane using interfacial polymerization for vanadium redox flow battery applications, *J. Membr. Sci.* 311 (2008) 98–103.
- [15] J.B. Liao, M.Z. Lu, Y.Q. Chu, J.L. Wang, Ultra-low vanadium ion diffusion amphoteric ion-exchange membranes for all-vanadium redox flow batteries, *J. Power Sources* 282 (2015) 241–247.
- [16] S. Winardi, S.C. Raghu, M.O. Oo, Q. Yan, N. Wai, T.M. Lim, M. Skyllas-Kazacos, Sulfonated poly(ether ether ketone)-based proton exchange membranes for vanadium redox battery applications, *J. Membr. Sci.* 450 (2014) 313–322.
- [17] W. Dai, L. Yu, Z. Li, J. Yan, L. Liu, J. Xi, X. Qiu, Sulfonated poly(ether ether ketone)/graphene composite membrane for vanadium redox flow battery, *Electrochim. Acta* 132 (2014) 200–207.
- [18] F. Wang, J.M. Sylvia, M.M. Jacob, D. Peramunage, Amphiphilic block copolymer membrane for vanadium redox flow battery, *J. Power Sources* 242 (2013) 575–580.
- [19] N. Wang, J. Yu, Z. Zhou, D. Fang, S. Liu, Y. Liu, SPPEK/TPA composite membrane as a separator of vanadium redox flow battery, *J. Membr. Sci.* 437 (2013) 114–121.
- [20] Z. Li, J. Xi, H. Zhou, L. Liu, Z. Wu, X. Qiu, L. Chen, Preparation and characterization of sulfonated poly(ether ether ketone)/poly(vinylidene fluoride) blend membrane for vanadium redox flow battery application, *J. Power Sources* 237 (2013) 132–140.
- [21] S. Macksasitorn, S. Changkhamchom, A. Sirivat, K. Siemanond, Sulfonated poly(ether ether ketone) and sulfonated poly(1,4-phenylene ether ether sulfone) membranes for vanadium redox flow batteries, *High Perform. Polym.* 24 (2012) 603–608.
- [22] C. Jia, J. Liu, C. Yan, A significantly improved membrane for vanadium redox flow battery, *J. Power Sources* 195 (2010) 4380–4383.
- [23] L. Semiz, N.D. Sankir, M. Sankir, Directly copolymerized disulfonated poly(arylene ether sulfone) membranes for vanadium redox flow batteries, *Int. J. Electrochem. Sci.* 9 (2014) 3060–3067.
- [24] B. Schwenzer, J. Zhang, S. Kim, L. Li, J. Liu, Z. Yang, Membrane development for vanadium redox flow batteries, *ChemSusChem* 4 (2011) 1388–1406.
- [25] D. Chen, S. Wang, M. Xiao, Y. Meng, Synthesis and properties of novel sulfonated poly(arylene ether sulfone) ionomers for vanadium redox flow battery, *Energy Convers. Manag.* 51 (2010) 2816–2824.
- [26] B. Yin, Z. Li, W. Dai, L. Wang, L. Yu, J. Xi, Highly branched sulfonated poly(flourenyl ether ketone sulfone)s membrane for energy efficient vanadium redox flow battery, *J. Power Sources* 285 (2015) 109–118.
- [27] L. Cao, Q. Sun, Y. Gao, L. Liu, H. Shi, Novel acid-base hybrid membrane based on amine-functionalized reduced graphene oxide and sulfonated polyimide for vanadium redox flow battery, *Electrochim. Acta* 158 (2015) 24–34.
- [28] J. Li, Y. Zhang, S. Zhang, X. Huang, Sulfonated polyimide/s-MoS₂ composite membrane with high proton selectivity and good stability for vanadium redox flow battery, *J. Membr. Sci.* 490 (2015) 179–189.
- [29] Y. Zhang, J. Li, H. Zhang, S. Zhang, X. Huang, Sulfonated polyimide membranes with different non-sulfonated diamines for vanadium redox battery applications, *Electrochim. Acta* 150 (2014) 114–122.
- [30] J. Li, Y. Zhang, L. Wang, Preparation and characterization of sulfonated polyimide/TiO₂ composite membrane for vanadium redox flow battery, *J. Solid State Electrochem.* 18 (2014) 729–737.
- [31] C. Fujimoto, S. Kim, R. Stains, X. Wei, L. Li, Z.G. Yang, Vanadium redox flow battery efficiency and durability studies of sulfonated Diels Alder poly(phenylene)s, *Electrochem. Commun.* 20 (2012) 48–51.
- [32] J. Qiu, L. Zhao, M. Zhai, J. Ni, H. Zhou, J. Peng, J. Li, G. Wei, Pre-irradiation grafting of styrene and maleic anhydride onto PVDF membrane and subsequent sulfonation for application in vanadium redox batteries, *J. Power Sources* 177 (2008) 617–623.
- [33] B. Zhang, E. Zhang, G. Wang, P. Yu, Q. Zhao, F. Yao, Poly(phenyl sulfone) anion exchange membranes with pyridinium groups for vanadium redox flow battery applications, *J. Power Sources* 282 (2015) 328–334.
- [34] W. Xu, Y. Zhao, Z. Yuan, X. Li, H. Zhang, I.F.J. Vankelecom, Highly stable anion exchange membranes with internal cross-linking networks, *Adv. Funct. Mater.* 25 (2015) 2583–2589.
- [35] C.W. Hwang, A.-H.-M. Park, C.M. Oh, T.-S. Hwang, J. Shim, C.-S. Jin, Synthesis and characterization of vinylimidazole-co-trifluoroethylmethacrylate-co-divinylbenzene anion-exchange membrane for all-vanadium redox flow battery, *J. Membr. Sci.* 468 (2014) 98–106.
- [36] H.-S. Choi, Y.-H. Oh, C.-H. Ryu, G.-J. Hwang, Characteristics of the all-vanadium redox flow battery using anion exchange membrane, *J. Taiwan Inst. Chem. Eng.* 45 (2014) 2920–2925.
- [37] C.-N. Sun, Z. Tang, C. Belcher, T.A. Zawodzinski, C. Fujimoto, Evaluation of Diels–Alder poly(phenylene) anion exchange membranes in all-vanadium redox flow batteries, *Electrochem. Commun.* 43 (2014) 63–66.
- [38] S.-J. Seo, B.-C. Kim, K.-W. Sung, J. Shim, J.-D. Jeon, K.-H. Shin, S.-H. Shin, S.-H. Yun, J.-Y. Lee, S.-H. Moon, Electrochemical properties of pore-filled anion exchange membranes and their ionic transport phenomena for vanadium redox flow battery applications, *J. Membr. Sci.* 428 (2013) 17–23.
- [39] P.K. Leung, Q. Xu, T.S. Zhao, L. Zeng, C. Zhang, Preparation of silica nanocomposite anion-exchange membranes with low vanadium-ion crossover for vanadium redox flow batteries, *Electrochim. Acta* 105 (2013) 584–592.
- [40] J. Fang, H. Xu, X. Wei, M. Guo, X. Lu, C. Lan, Y. Zhang, Y. Liu, T. Peng, Preparation and characterization of quaternized poly(2,2,2-trifluoroethyl methacrylate-co-N-vinylimidazole) membrane for vanadium redox flow battery, *Polym. Adv. Technol.* 24 (2013) 168–173.
- [41] Z. Mai, H. Zhang, H. Zhang, W. Xu, W. Wei, H. Na, X. Li, Anion-conductive membranes with ultralow vanadium permeability and excellent performance in vanadium flow batteries, *ChemSusChem* 6 (2013) 328–335.
- [42] S. Zhang, C. Yin, D. Xing, D. Yang, X. Jian, Preparation of chloromethylated/quaternized poly(phthalazinone ether ketone) anion exchange membrane materials for vanadium redox flow battery applications, *J. Membr. Sci.* 363 (2010) 243–249.
- [43] H. Vogel, C.S. Marvel, Polybenzimidazoles, new thermally stable polymers, *J. Polym. Sci. L* (1961) 511–539.
- [44] H. Xu, K. Chen, X. Guo, J. Fang, J. Yin, Synthesis of novel sulfonated poly-

- benzimidazole and preparation of cross-linked membranes for fuel cell application, *Polymer* 48 (2007) 5556–5564.
- [45] N. Xu, X. Guo, J. Fang, H. Xu, J. Yin, Synthesis of novel polybenzimidazoles with pendant amino groups and the formation of their crosslinked membranes for medium temperature fuel cell applications, *J. Polym. Sci.* 47 (2009) 6992–7002.
- [46] X.L. Zhou, T.S. Zhao, L. An, L. Wei, C. Zhang, The use of polybenzimidazole membranes in vanadium redox flow batteries leading to increased coulombic efficiency and cycling performance, *Electrochim. Acta* 153 (2015) 492–498.
- [47] J. Qiu, M. Li, J. Ni, M. Zhai, J. Peng, L. Xu, H. Zhou, J. Li, G. Wei, Preparation of ETFE-based anion exchange membrane to reduce permeability of vanadium ions in vanadium redox battery, *J. Membr. Sci.* 297 (2007) 174–180.
- [48] H.-Z. Zhang, H.-A. Zhang, X. Li, Z. Mai, W. Wei, Silica modified nanofiltration membranes with improved selectivity for redox flow battery application, *Energy Environ. Sci.* 5 (2012) 6299–6303.
- [49] R. Bouchet, E. Siebert, Proton conduction in acid doped polybenzimidazole, *Solid State Ion.* 118 (1999) 287–299.
- [50] J.A. Asensio, S. Borros, P. Gomez-Romero, Proton-conducting polymers based on benzimidazoles and sulfonated benzimidazoles, *J. Polym. Sci. Part A Polym. Chem.* 40 (2002) 3703–3710.
- [51] X. Xu, L. Li, H. Wang, X. Li, X. Zhuang, Solution blown sulfonated poly(ether ether ketone) nanofiber–Nafion composite membranes for proton exchange membrane fuel cells, *RSC Adv.* 5 (2015) 4934–4940.
- [52] X. Luo, Z. Lu, J. Xi, Z. Wu, W. Zhu, L. Chen, X. Qiu, Influences of permeation of vanadium ions through PVDF-g-PSSA membranes on performances of vanadium redox flow batteries, *J. Phys. Chem. B* 109 (2005) 20310–20314.
- [53] C. Sun, J. Chen, H. Zhang, X. Han, Q. Luo, Investigations on transfer of water and vanadium ions across Nafion membrane in an operating vanadium redox flow battery, *J. Power Sources* 195 (2010) 890–897.